Bonding and Reactivity in the Electronically Unsaturated Hydrogen-Bridged Dimer [Ru3(CO)8(μ3-CMe)(μ-H)2(μ3-H)]2

ARTICLE *in* ORGANOMETALLICS · DECEMBER 2011

Impact Factor: 4.13 · DOI: 10.1021/om2012375

ORGANOMETALLICS

Communication

pubs.acs.org/Organometallics

Bonding and Reactivity in the Electronically Unsaturated Hydrogen-Bridged Dimer $[Ru_3(CO)_8(\mu_3\text{-CMe})(\mu\text{-H})_2(\mu_3\text{-H})]_2$

Richard D. Adams,*[†] Yuwei Kan,[†] Qiang Zhang,[†] Michael B. Hall,*[‡] and Eszter Trufan[‡]

[†]Department of Chemistry and Biochemistry, University of South Carolina, Columbia, South Carolina 29208, United States

[‡]Department of Chemistry, Texas A & M University, College Station, Texas 77843, United States

Supporting Information

ABSTRACT: The electronically unsaturated complex $[Ru_3(CO)_8(\mu_3\text{-CMe})(\mu\text{-H})_2(\mu_3\text{-H})]_2$ (**1**), viewed as a dimer of the 46-electron fragment $Ru_3(CO)_8(\mu_3\text{-CMe})(\mu\text{-H})_3$, is held together by delocalized bonding involving two triply bridging hydride ligands. Compound **1** exhibits a dynamic activity in solution that equilibrates two of the three types of hydride ligands. Compound **1** reacts with 1,1-bis(diphenylphosphino)methane to form the macrocyclic complex $[Ru_3(CO)_7(\mu_3\text{-CMe})(\mu\text{-H})_3]_2(\mu\text{-dppm})_2$ (**3**).

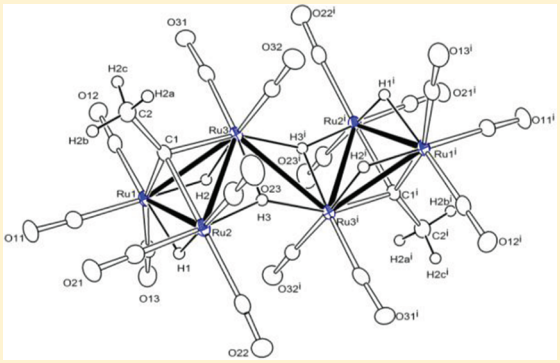

Electronic unsaturation in chemical compounds can be expressed in a variety of ways. It is readily recognized in the form of "empty" valence orbitals, such as the one found on the boron atom in BF_3, or in multiple bonds, as found in alkenes and alkynes.[1] In metal complexes it can be found in the form of empty orbitals at a "vacant" coordination site[2] or in metal−metal multiple bonds.[3] In the presence of hydrogen, unsaturation can be disguised by the formation of delocalized bonds having hydrogen bridges as found in boranes, such as B_2H_6,[4] or in polynuclear metal complexes, such as the 46-electron triosmium complex $Os_3(CO)_{10}(\mu\text{-H})_2$[5] (**A**), the 56-electron tetrarhenium complex $Re_4(CO)_{12}(\mu\text{-H})_4$[6] (**B**), and higher clusters such as the five-metal 68-electron complex $Pt_2Re_3(CO)_9(PR)_3(\mu\text{-H})_6$ (**C**, R = tBu_3).[7,8]

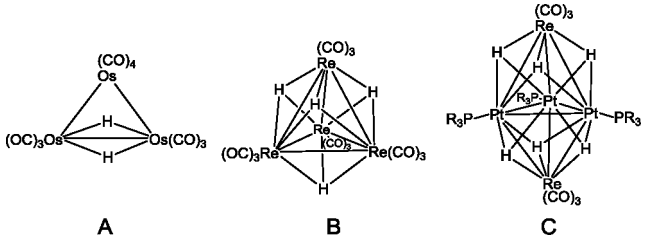

A B C

Herein we describe a new form of this hydrogen-bridged unsaturation which is located in the linkage between two triruthenium carbonyl clusters in the hexaruthenium carbonyl complex $[Ru_3(CO)_8(\mu_3\text{-CMe})(\mu\text{-H})_2(\mu_3\text{-H})]_2$ (**1**).

Compound **1** was obtained by a silica gel induced decarbonylation of the 48-electron complex $Ru_3(CO)_9(\mu_3\text{-CMe})(\mu\text{-H})_3$ (**2**)[9,10] and was characterized by a low-temperature single-crystal X-ray diffraction analysis. An ORTEP diagram of the molecular structure of compound **1** is shown in Figure 1.

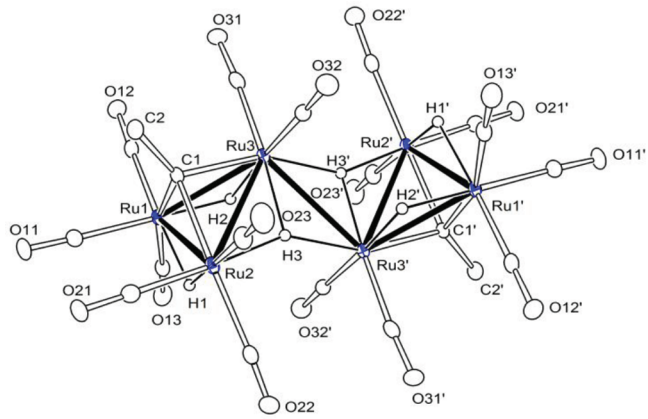

Figure 1. An ORTEP diagram of the molecular structure of $Ru_6(CO)_{16}(\mu_3\text{-CMe})_2(\mu\text{-H})_4(\mu_3\text{-H})_2$ (**1**), showing thermal ellipsoids at the 30% probability level. Selected interatomic bond distances (Å) are as follows: Ru(1)−Ru(3) = 2.8544(4), Ru(1)−Ru(2) = 2.8650(3), Ru(2)−Ru(3) = 2.8840(3), Ru(3)−Ru(3′) = 2.9932(5), Ru(2)−Ru(3′) = 3.627(1), Ru(1)−C(1) = 2.094(3), Ru(2)−C(1) = 2.097(3), Ru(3)−C(1) = 2.032(3), Ru(1)−H(1) = 1.78(4), Ru(1)−H(2) = 1.69(4), Ru(2)−H(1) = 1.82(4), Ru(2)−H(3) = 1.81(3), Ru(3)−H(2) = 1.88(4), Ru(3)−H(3) = 1.85(4).

The compound can be viewed as a centrosymmetrically coupled dimer of two 46-electron triruthenium fragments "$Ru_3(CO)_8(\mu_3\text{-CMe})(\mu\text{-H})_3$", each formed by the loss of one CO ligand from a molecule of **2**. The two Ru_3 clusters are linked by a long, hydrogen-bridged metal−metal bond:

Received: December 13, 2011
Published: December 21, 2011

   dx.doi.org/10.1021/om2012375 | *Organometallics* 2012, 31, 50−53

Ru(3)−Ru(3′) = 2.9932(5) Å. The Ru−Ru bonds within the Ru_3 triangles are shorter, Ru(1)−Ru(3) = 2.8544(4) Å, Ru(1)−Ru(2) = 2.8650(3) Å, and Ru(2)−Ru(3) = 2.8840(3) Å, and are similar to those found in **2**, 2.841(6) and 2.844(6) Å.[11] As in **2**, each Ru−Ru bond within the Ru_3 triangles contains a bridging hydrido ligand (located and refined in the structural analysis), but two of these, H(3) and H(3′), serve as triply bridging ligands by extending to the ruthenium atom, Ru(3), in the neighboring Ru_3 triangle. The Ru(2)···Ru(3′) distance between the two Ru_3 clusters, 3.627(1) Å, is too long for a direct bonding interaction.

Compound **1** contains a total of 92 valence electrons. A six-metal cluster with seven metal−metal bonds should have 94 electrons, (6 × 18) − (7 × 2), if all of the metal atoms formally have an 18-electron configuration.[12] In order to obtain a clearer picture of bonding in **1**, several DFT calculations have been performed: first, a geometry optimization starting with the structure as found in the solid state, followed by a vibrational frequency calculation to confirm the stationary point as a minimum, and then a fragment analysis to help explain the bonding (details are given in the Supporting Information). To better understand the stability of the dimer, **1**, DFT calculations were also performed on the two $Ru_3(CO)_8(\mu_3\text{-CMe})(\mu\text{-H})_3$ monomer units of **1**, and the proposed intermediate that contains the direct Ru(3)−Ru(3′) bond, but without triply bridging H(3) or H(3′) ligands. The details of the optimized structures for these three species are shown in Figure 2. Our

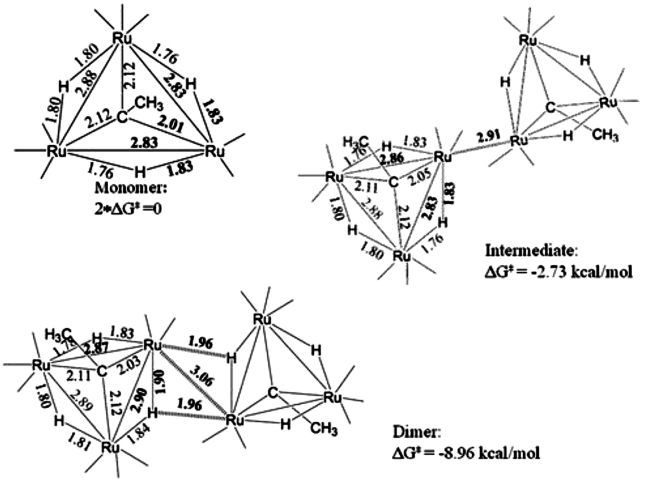

Figure 2. Schematic representations of the monomer, the intermediate with the Ru(3)−Ru(3′) bond, and the dimer, showing bond distances of the optimized structures and the relative Gibbs free energies of the systems.

analysis shows that the combination of the two $Ru_3(CO)_8(\mu_3\text{-CMe})(\mu\text{-H})_3$ units to form the intermediate with only the Ru(3)−Ru(3′) bond lowers the Gibbs free energy (ΔG°) of the system by 2.73 kcal/mol and creates a metal−metal bond at 2.91 Å. The rearrangement of this structure into the observed dimer with contributions from the triply bridging H(3) and H(3′) lowers the ΔG° of the system to 8.96 kcal/mol below that of the two monomers and lengthens the Ru(3)−Ru(3′) bond to 3.06 Å. These results indicate that the Ru(3)−Ru(3′), H(3)−Ru(3′), and H(3′)−Ru(3) interactions all contribute to the bonding in **1**.

The fragment analysis describes the nature of the bonding between two monomers (labeled A and B) that are frozen in the geometry that they display in the optimized dimer structure, rather than at their independently optimized geometry as described above. These calculations show that the total (intrinsic) electronic bond energy of −33.40 kcal/mol is comprised mostly of orbital interactions (−31.58 kcal/mol) and a small contribution (−1.82 kcal/mol) from the sum of the electrostatic (attraction in this case) and Pauli repulsions. The source of this orbital stabilization is mixing of the LUMO of each monomer fragment with several occupied fragment orbitals, specifically the HOMO-2, HOMO-8, and HOMO-11, of the other fragment. The key features of this mixing are described below, and related orbital contour drawings are shown in Figure 3. The most significant pair of interactions

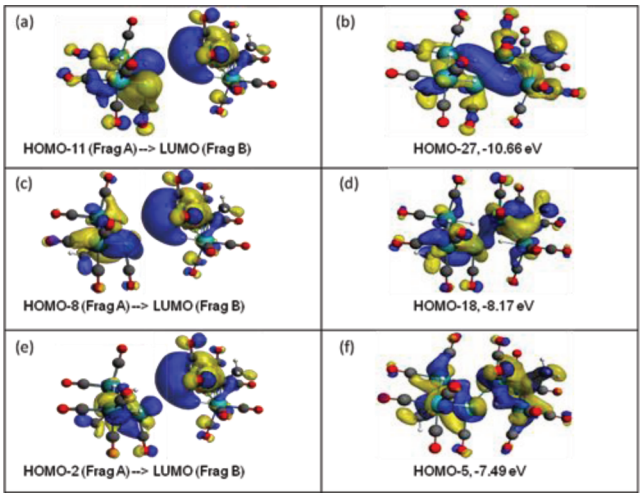

Figure 3. Orbital contour diagrams at the isosurface value of 0.03 for the fragment orbitals and 0.02 for the dimer orbitals showing (a) HOMO-11 of fragment A (the electron-donor orbital) in relation to the LUMO of fragment B (the electron-acceptor orbital), (b) HOMO-27, the major MO making a net contribution to the bonding between the two fragments in the dimer **1**, (c) HOMO-8 of fragment A (the electron-donor orbital) in relation to the LUMO of fragment B (the electron-acceptor orbital), (d) HOMO-18, a MO making a net contribution to the bonding between the two fragments in the dimer **1**, (e) the HOMO-2 of fragment A (the electron-donor orbital) in relation to the LUMO of fragment B (the electron-acceptor orbital), and (f) HOMO-5, the second most important MO making a net contribution to the bonding between the two fragments in the dimer **1**. Note that the orientation has the bridging Ru atoms upper right and lower left.

occurs when the LUMO of one of the monomer fragments accepts electron density from the HOMO-11 of the other fragment, as shown in Figure 3a for one of the pairs. This mixing leads to significant bonding in the HOMO-27 of the dimer **1**, as shown in Figure 3b. The HOMO-8 of each fragment has a similar, but somewhat weaker, interaction with the LUMO of the other fragment, as shown in Figure 3c. This second interaction enhances the bonding in the HOMO-18 of the dimer **1**, shown in Figure 3d. Finally, the LUMO of each fragment also mixes with the HOMO-2 of the other fragment (Figure 3e), in a way that enhances the bonding from the HOMO-5 of **1**, shown in Figure 3f.

The unsaturation of the monomer fragment is concentrated in the LUMO, which is the orbital that a two-electron-donor ligand such as a carbonyl or a phosphine would use to make an additional bond. In the dimer **1**, the unsaturation is resolved by electron donation from the HOMO-11, HOMO-8, and

dx.doi.org/10.1021/om2012375 | *Organometallics* 2012, 31, 50−53

HOMO-2 orbitals of the other fragment. Thus, the dimer has both triply bridging H's and direct Ru(3)−Ru(3′) bonding.

Variable-temperature ^{1}H NMR spectra of the hydride ligands in **1** show that the compound is dynamically active in solution. At low temperature (−90 °C), the spectrum exhibits three resonances at −16.51 (br, 2H), −16.96 (s, 2H) and −20.68 ppm (br, 2H) for each of the three types of bridging hydride ligands, which is in accord with the structure found in the solid state. However as the temperature is raised, the two broad resonances at −16.51 and −20.68 ppm broaden further and merge into a single peak, which is sharp at −18.30 ppm at room temperature (see Figure S2 in the Supporting Information). These changes can be explained by a rocking rearrangement motion in which the environments of the triply bridging hydride ligands H(3) are exchanged in a pairwise fashion with the pair of edge-bridging hydride ligands H(2), but they are not exchanged with the other bridging hydride ligands H(1), as shown in Scheme 1 (CO labels are not shown in Scheme 1).

Scheme 1. Dynamic Rearrangement of 1 in Solution

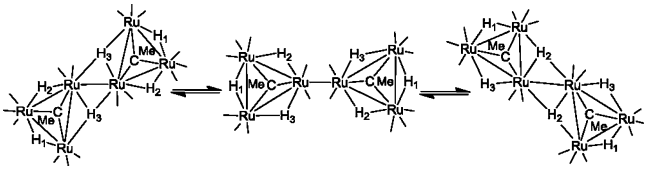

Alternatively, the molecule could simply dissociate into two $Ru_3(CO)_8(\mu_3\text{-CMe})(\mu\text{-H})_3$ fragments and then recombine in such a way that H(2) and H(3) have been interchanged. Lineshape analyses have provided the following activation parameters: $\Delta H^{\ddagger}$ = 8.7(5) kcal/mol, $\Delta S^{\ddagger}$ = 2.5 cal/K. The small value of $\Delta S^{\ddagger}$ would suggest a nondissociative mechanism.

Electronically unsaturated compounds generally exhibit higher reactivity than saturated compounds. Such is also the case with **1**. When treated with CO at room temperature, compound **1** was rapidly converted back to **2**, quantitatively. When treated with 1,1-bis(diphenyphosphino)methane (dppm), compound **1** was converted to the new compound $[Ru_3(CO)_7(\mu_3\text{-CMe})(\mu\text{-H})_3]_2(\mu\text{-dppm})_2$ (**3**) in 25% yield at room temperature within 5 min. Compound **3** was characterized structurally by a single crystal X-ray diffraction analysis, and an ORTEP diagram of its molecular structure is shown in Figure 4.

Compound **3** is a centrosymmetrical dimer linked by two bridging dppm ligands; each phosphorus atom of the dppm is coordinated to a different Ru_3 cluster. The hydrogen-bridged link between the two triruthenium clusters of **1** was completely ruptured and a 10-membered macrocycle which contains two dppm-substituted triruthenium clusters was created in its place (see Scheme 2). The Ru−Ru bonding within each Ru_3 triangle, Ru(1)−Ru(3) = 2.8533(14) Å, Ru(1)−Ru(2) = 2.8710(13) Å, and Ru(2)−Ru(3) = 2.8445(15) Å, is similar to that in **2**.[11]

Notably, there was no formation of compound **3** in the reaction between compound **2** and dppm at room temperature in 2 h, although after 20 h, one is able to isolate instead the chelate complex $Ru_3(CO)_7(\mu_3\text{-CMe})(\mu\text{-H})_3(\mu\text{-dppm})$ (**4**) in 31% yield (see Scheme 3 and Figure S3 in the Supporting Information).

Other molecules with unsaturation such as **1** may exist as intermediates or even as isolable compounds in decarbonylation reactions involving hydride containing metal carbonyl

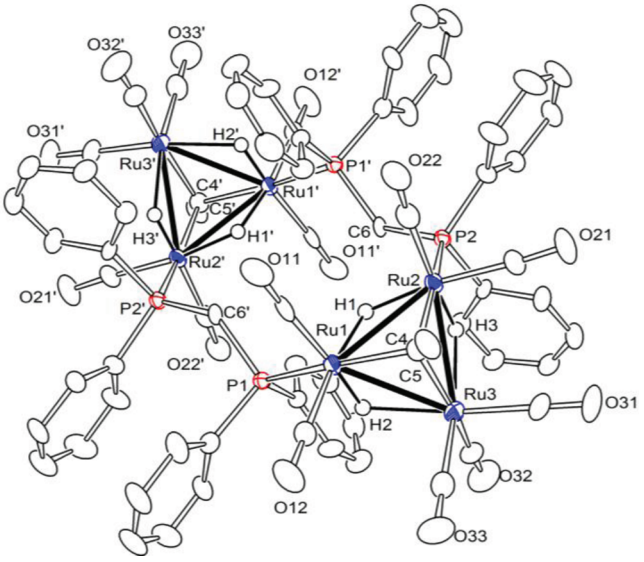

Figure 4. ORTEP diagram of the molecular structure of $[Ru_3(CO)_7(\mu_3\text{-CMe})(\mu\text{-H})_3]_2(\mu\text{-dppm})_2$ (**3**), showing thermal ellipsoids at the 20% probability level. Selected interatomic bond distances (Å) are as follows: Ru(1)−Ru(3) = 2.8533(14), Ru(1)−Ru(2) = 2.8710(13), Ru(2)−Ru(3) = 2.8445(15), Ru(1)−C(4) = 2.071(11), Ru(2)−C(4) = 2.054(13), Ru(3)−C(4) = 2.072(15), Ru(1)−P(1) = 2.436(3), Ru(2)−P(2) = 2.451(3), Ru(1)−H(1) = 1.67(10), Ru(1)−H(2) = 1.38(14), Ru(2)−H(1) = 1.70(10), Ru(2)−H(3) = 1.33(15), Ru(3)−H(3) = 1.95(16), Ru(3)−H(2) = 2.04(13).

Scheme 2. Formation of 3 from 1

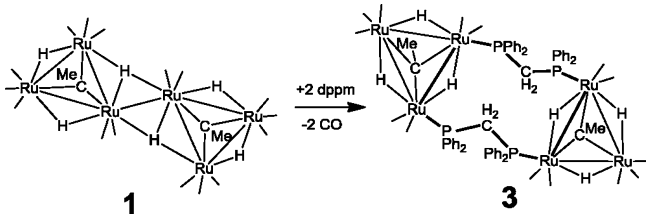

Scheme 3. Formation of 4 from 2

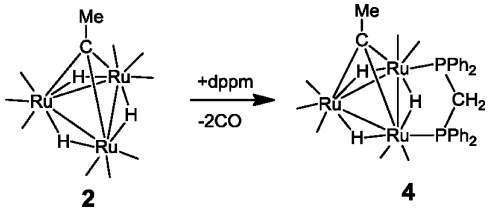

cluster complexes. One such species is the hexaruthenium complex $Ru_6(CO)_{14}[\mu_4\text{-}\eta^2\text{-}OCH_2CHNC(Me)OC(Ph)]_2(\mu_3\text{-H})_2$, which is held together in part by two bridging hydride ligands and two polydentate bridging oxazoline ligands.[13]

■ ASSOCIATED CONTENT

Supporting Information

Text, tables, figures, and CIF files giving experimental details, characterization data, and crystal data for the structural analyses. This material is available free of charge via the Internet at http://pubs.acs.org.

dx.doi.org/10.1021/om2012375 | *Organometallics* 2012, 31, 50−53

AUTHOR INFORMATION

Corresponding Author

*E-mail: adams@chem.sc.edu (R.D.A.); hall@science.tamu.edu (M.B.H.).

ACKNOWLEDGMENTS

This research was supported by the National Science Foundation (Grant No. CHE-1111496, R.D.A.). The authors from Texas A&M University gratefully acknowledge the National Science Foundation (Grant Nos. CHE-0541587 and CHE-0910552) and The Welch Foundation (Grant No. A-0648) for support.

ABBREVIATIONS

LUMO, lowest unoccupied molecular orbital; HOMO, highest occupied molecular orbital; ORTEP, Oak Ridge thermal ellipsoid plot; DFT, density functional theory

REFERENCES

(1) Gimarc, B. M. *Acc. Chem. Res.* **1974**, *7*, 384−392.
(2) (a) Crabtree, R. H. *The Organometallic Chemistry of the Transition Metals*, 4th ed.; Wiley-Interscience: Hoboken, NJ, 2005; p 56. (b) Collman, J. P. *Trans. N. Y. Acad. Sci.* **1968**, 479−482.
(3) Schaefer, H. F. III; King, R. B. *Pure Appl. Chem.* **2001**, *73*, 1059−1073.
(4) Trinquier, G.; Malrieu, J. P.; Garciacuesta, I. *J. Am. Chem. Soc.* **1991**, *113*, 6465−6473.
(5) Broach, R. W.; Williams, J. M. *Inorg. Chem.* **1979**, *18*, 314−319.
(6) Wilson, R. D.; Bau, R. *J. Am. Chem. Soc.* **1976**, *98*, 4687−4689.
(7) Adams, R. D; Captain, B.; Beddie, C.; Hall, M. B. *J. Am. Chem. Soc.* **2007**, *129*, 986−1000.
(8) Electronically saturated metal cluster complexes have the following valence electron counts: 48 for triangles with three metal atoms, 60 for a tetrahedron of four metal atoms, and 72 for a trigonal-bipyramidal cluster of five metal atoms.
(9) Yellow **2** decomposes to orange **1** (48% yield) within a few minutes when placed on silica gel in air. Compound **1** also decomposes on silica gel, but more slowly than that of **2**. Compound **1** can be isolated by rapid removal from the silica gel with a final purification by recrystallization. It is fairly air stable in the solid state. For further details see the accompanying Supporting Information.
(10) Canty, A. J.; Johnson, B. F. G.; Norton, J. R.; Lewis, J. *J. Chem. Soc., Chem. Commun.* **1972**, 1331−1332.
(11) Sheldrick, G. M.; Yesinowski, J. P. *J. Chem. Soc., Dalton Trans.* **1975**, 873−876.
(12) Wade, K. In *Transition Metal Clusters*; Johnson, B. F. G., Ed.; Wiley: Chichester, U.K., 1980; Chapter 3, pp 209−264.
(13) Bhaduri, S.; Sapre, N.; Jones, P. G. *J. Organomet. Chem.* **1996**, *509*, 105−107.